PR5 Studies on Actinides and Fission Products Performed at the KURRI Hot Laboratory

T. Fujii

Research Reactor Institute, Kyoto University

1. Objectives and Allotted Research Subjects

Studies on actinide and fission product nuclides with careful management are being more important for reprocessing, disposal, partitioning, and transmutation processes in the nuclear fuel cycle. Hot laboratory of KURRI is one of core facilities in Japan, in which various nuclides can be handled. This project enhances utilization of the KURRI hot laboratory by opening for fundamental and application studies related to radiochemistry, nuclear chemistry, environmental chemistry, geochemistry, and so on. Allotted research subjects are;

ARS-1 Complexation of actinides with organic substances (T. Sasaki *et al*.).

ARS-2 Solubility of actinide compounds in aqueous media (T. Kobayashi *et al*.).

ARS-3 Leaching of actinides and FPs from fuel debris (N. Sato *et al*.).

ARS-4 Neutron irradiation damage of vitrified waste matrices (T. Nagai *et al*.).

ARS-5 Ligand exchange reaction of actinides in molten salts (A. Uehara *et al*.).

ARS-6 Electrochemical behavior of uranium in pyroreprocessing system (Y. Sakamura *et al*.).

ARS-7 Structural study of f-elements in molten halides (H. Matsuura *et al*.).

ARS-8 Molecular dynamics simulation of uranyl ion in molten salts (N. Ohtori *et al*.).

ARS-9 Fundamental study of fission products for trans-actinide chemistry (Y. Kasamatsu *et al*.).

ARS-10 Isotope separation by using microreactor (R. Hazama *et al*.).

ARS-11 Optical properties of molten aluminum halides (T. Goto *et al*.).

ARS-12 Precipitation of f-element oxides in molten halides (H. Sekimoto *et al*.).

ARS-13 Uptake of radiocesium and radiopotassium in plants (T. Ohta *et al*.).

ARS-14 Quantitative analysis of radionuclides in seawater (T. Kubota *et al*.).

ARS-15 Isotopic composition of radionuclides in environmental samples (Y. Shibahara *et al*.).

ARS-16 Noble gas mass spectrometry of neutron irradiated geological samples (H. Sumino *et al*.).

ARS-17 $^{40}Ar/^{39}Ar$ dating of neutron irradiated minerals and glasses (O. Ishizuka *et al*).

ARS-18 Radiometric Ar-Ar dating of neutron irradiated lavas (N. Hirano *et al*.).

ARS-19 Behavior of fission products in soil samples (S. Fukutani *et al*.).

2. Main Results and Contents

ARS-1, 2, 3, and 4 were performed in order to deepen the knowledge of nuclear waste management issues. In ARS-1, for understanding the randomly cross-linked heterogeneous and macromolecule properties of humic substances (HSs), the complexation of actinides with HS was studied. The HS samples irradiated by Co-60 gamma-ray source at KURRI were characterized by NMR measurement, and the dependence of dose rate on the chemical structure was clarified. ARS-2 studied on the solid phase transformation of $Th(OH)_4$(am: amorphous) at 363 K. The apparent solubility and particle size of the solid phase after aging were evaluated. ARS-5, 6, 7, 8, and 12 were performed with the viewpoint of pyrochemistry. In ARS-5, the solubility of uranium in various molten alkali chlorides was determined. It was found that the solubility of uranium does not depend on the melting point of molten salts but increases with ionic diameter of solvent alkali metal ion. ARS-6 studied on the behavior of Al^{3+} in LiCl-KCl eutectic melt in order to develop the separation technique of Al from Al-actinides intermetallic compounds. It was found that Al can be separated from U by using a Cu electrode in LiCl-KCl melts. In ARS-7, the electrochemical measurement of zircomium in molten LiCl-KCl has been carried out for the first step of the elucidation of electrochemical behavior containing zircomium. The results suggested that zirconium would be difficult to be selectively electoreduced in molten LiCl-KCl depending on the concentration of zircomium. In ARS-8, the Helmholtz free energy changes for the successive additional processes of chloride ion to uranyl ion in aqueous solutions of LiCl with various concentrations have been evaluated. The stability of uranyl ion in hydrate melts was then discussed. ARS-12 studied on the formation of Nd(II), Dy(II) and Pr(II) in $CaCl_2$-LiCl eutectic molten salt with the combination of the absorption spectroscopy and the galvanostatic electrolysis method. The results showed that Nd(II) was decomposed through the disproportionation reaction. ARS-10 studied isotope fractionation of Ca. A possible fractionation of $^{48}Ca/^{40}Ca$ was found. ARS-13, 14, 15, 16, 17, and 18 focus on environmental chemistry and geochemistry by using KUR.

3. Summaries of the achievements

New and characteristic chemical, kinetic, structural, and thermodynamic data for actinides and fission products were obtained. These new information encompass solid chemistry, molten salt and solution chemistry, as well as nuclear reactions of f-elements and FPs. Restart of the KUR operation is strongly awaited.

27P5

PR5-1 Study on Chemical Property of Gamma-irradiated Natural Organic Matters

T. Sasaki, T. Kobayashi, S. Nishikawa, R. Goto,
A. Uehara[1], T. Fujii[1] and T. Saito[1]

Graduate School of Engineering, Kyoto University
[1]Research Reactor Institute, Kyoto University

INTRODUCTION: Due to the randomly cross-linked heterogeneous and macromolecule properties of humic substances (HSs) as natural organic matter, in soils, sediments, and natural waters, the apparent formation constant of actinides with HS changes depending on the solution conditions such as pH, metal and HS concentrations, and ionic strength. When the HS in underground water contacts with a radioactive waste package at repository site, the chemical property of HS should be altered by gamma-irradiation and the ability of complex formation may be decreased. The HS samples irradiated by Co-60 gamma-ray source at KURRI were characterized by NMR measurement, and the dependence of dose rate on the chemical structure was discussed.

EXPERIMENTS: The Eliot soil humic acid (SHA, 1S102H) and Suwannee river fulvic acid (SFA, 1S101F) were purchased from International Humic Substance Society (IHSS). The proton dissociation constants have been reported. The brownish aqueous solution samples for Co-60 gamma-irradiation were prepared to be 10^{-3} eq/dm^3 at a given alkaline pH condition. The irradiation dose were 10, 100 and 500 kGy by controlling the time of exposure. ^{1}H NMR spectrum was obtained at 600.17 MHz (JEOL JNM-ECA600 FT NMR spectrometer) with acquisition time of 1.45 sec, pulse delay time of 5 sec, and accumulation of 1000 scans, and ^{13}C NMR spectrum was obtained at 600.17 MHz with acquisition time of 0.69 sec, pulse delay time of 10 sec, and accumulation of 24000 scans.

RESULTS: The blackish precipitation was observed in the SHA solution after 500 kGy irradiation, and the same irradiation achromatized the SFA solution, suggesting a different degradation process. As shown in Fig. 1, the proton NMR spectra of HS have broad peaks at the entire chemical shift range and are different from that of general and commercially available reagents such as acetic acid and EDTA. Based on the previous studies about natural hydrocarbon compounds [1-4], these peaks of ^{1}H were assigned to be some kinds of functional groups. The integrated intensity of peaks is summarized in Table 1. The fragment of aliphatic hydrocarbon Hγ increased after 10 kGy irradiation, while that of the aromatic protons H_{Ar} decreased. Meanwhile, the S/N ratio of ^{13}C NMR spectra was significant low even in longer acquisition time. For better understanding of chemical property, a higher performance of NMR would need for further study.

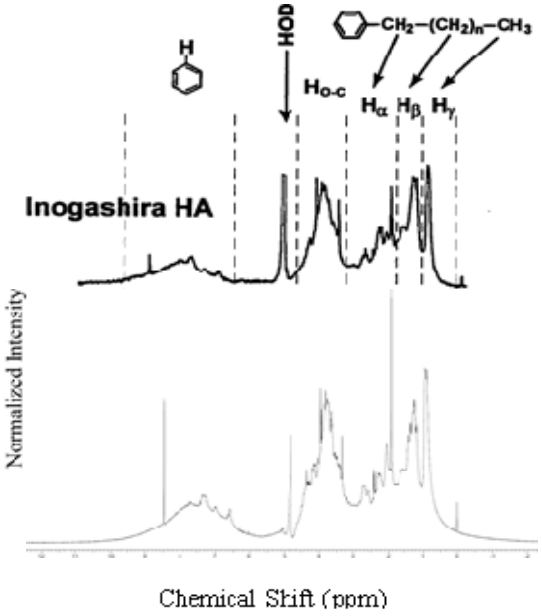

Fig. 1. ^{1}H NMR spectra of un-irradiated Eliot soil humic acid (1S102H). (600.17MHz, Number of transients:1000) The upper spectrum of Inogashira-HS is obtained from ref [5] for comparison.

Table 1. Distribution% of protons in SHA based on the ^{1}H peak area at each range of chemical shift.

Dose (kGy)	Proton assigned (δ, ppm)				
	Hγ (0-0.9)	Hβ (0.9-1.6)	Hα (1.6-3.0)	H_{O-C} (3.0-4.3)	H_{Ar} (6.0-9.0)
0	7.8	16.7	23.3	33.3	18.9
10	10.8	16.9	22.9	32.5	16.9

REFERENCES:

[1] H. Oka et al. *Nenryo Kyokaishi* (*J. Jpn. Fuel Soc.*), 48 (1969) 295-302.
[2] K. Yonebayashi and T. Hattori, *Soil Sci. Plant Nutr.*, 35 (1989) 383-392.
[3] R.D. Malcolm, *Anal. Chem. Acta*, 232 (1990) 19-30.
[4] M. Kawahigashi et al., *Soil Sci. Plant Nutr.*, 42 (1996) 355- 360.
[5] A. Watanabe, K. Tsutsuki, S. Kuwatsuka, *Sci. Total Environm.*, 81/82 (1989) 195-200.

PR5-2

Effect of Solid Phase Transformation on the Solubility Product of Thorium Hydrous Oxide at 363 K

T. Kobayashi, H. Mizukoshi, T. Sasaki, A. Uehara[1] and T. Fujii[1]

Graduate School of Engineering, Kyoto University
[1]Research Reactor Institute, Kyoto University

INTRODUCTION: In the repository systems for high-level wastes or spent nuclear fuels, decay heat emissions are transferred to the groundwater aquifers surrounding the waste packages. Although the actual operating temperature depends on the structure of the repository system, temperature conditions greater than 333 K are thought to simulate results of temperature evolution up to a thousand years [1]. For evaluating the effects of the possible temperature on tetravalent actinide (An(IV)) migration behavior under certain scenarios, such as early failure of the waste package, it is necessary to determine the temperature effect on An(IV) solubility.
Under geological disposal conditions, An(IV) solubility is primarily controlled by amorphous hydroxide solid phase ($An(OH)_4$(am)). However, $An(OH)_4$(am) is thermodynamically meta-stable, and it is converted to stable crystalline oxides (AnO_2(cr)) by heating and calcination. A transformation of $An(OH)_4$(am) into a solid phase with higher crystallinity has also been shown to occur in aqueous solutions at high temperatures [2]. These observations indicate that the thermodynamic description of An(IV) solubility under elevated temperatures requires clarification of a possible transformation of $An(OH)_4$(am) as a solubility-limiting solid phase.
In the present study, we focused on the solid phase transformation of $Th(OH)_4$(am) at 363 K. Sample solutions in contact with $Th(OH)_4$(am) were stored in a chamber controlled at the aging temperature of 363 K. The apparent solubility and particle size of the solid phase after aging at 363 K were then investigated.

EXPERIMENTS: A 0.3 M ^{232}Th stock solution diluted to obtain sample solutions, and pH value was adjusted by $HClO_4$/NaOH. The sample solutions were kept in an oven controlled at 363 K for given periods. After aging, the sample solutions cooled down to 298 K and the pH values measured. The apparent solubility was measured by inductively coupled plasma mass spectroscopy (ICP-MS; HP4500, Hewlett Packard) after ultrafiltration (3k - 100k Da filter, Millipore), and the solubility product was determined. The detection limit for ICP-MS was about 10^{-8} M. The solid phases after aging at 363 K were separated, and then investigated using XRD (RINT 2000, RIGAKU). The Scherrer equation was applied to the XRD patterns to determine the particle size of the solid phases.

RESULTS: Th(IV) solubility after heating at 363 K for 7 days started to decrease and the values after 41 days were approximately 3 orders of magnitude lower than those of $Th(OH)_4$(am). In the XRD spectra of the solid phases kept at 363 K, broad peaks corresponding to ThO_2(cr) were observed, indicating a progress of the crystallization of initial $Th(OH)_4$(am).
In Figure 1, trends of the solubility product for different Th solid phases are shown as a function of particle size [3]. A dotted line represents an estimated solubility product according to the Schindler equation [4]. The solubility product value obtained in this study seems to be consistent with general trends of the data, but is much lower than the values for $Th(OH)_4$(am,fresh) and $Th(OH)_4$(am,dried), in spite of similar particle sizes. The observed difference might be explained by considering the higher sensitivity of the solubility value on the size of the smaller solid particles, and by considering possible differences in the size distributions of solid particles prepared by different experimental methods

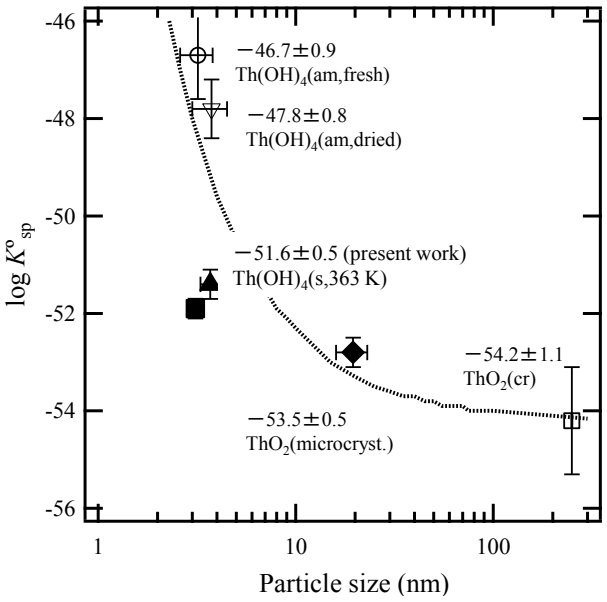

Fig. 1. The effect of particle size on the solubility product of $Th(OH)_4$(s,363) compared with the different solid phases and predicted curves from the Schindler equation [3].

REFERENCES:

[1] 2nd progress report on research and development for the geological disposal of HLW in Japan, JNC Report TN1410 2000-001, JNC, Tokai, Japan.
[2] D. Rai *et al.* Radiochim. Acta **88**, (2000) 297.
[3] T. Kobayashi et al., J. Nucl. Sci. Technol. In press. (2016).
[4] M. Rand *et al*. Chemical Thermodynamics of Thorium. Elsevier, Amsterdam; 2009.

PR5-3

Solubility of Uranium (VI) Oxides in High Temperature Molten Alikali Chlorides

A. Uehara, T. Nagai[1] and T. Fujii

[1] *Research Reactor Institute, Kyoto University*
[2] *Nuclear Fuel Cycle Engineering Lab., Japan Atomic Energy Agency*

INTRODUCTION:

In the non-aqueous reprocessing process of spent nuclear fuels by the pyrometallurgical and the electrowinning methods, a spent fuel is dissolved into molten alkali metal chloride eutectic and uranium and plutonium ions are recovered as metal or oxide. In the present study, the solubility of uranium ions in various kinds of molten alkali chlorides was measured.

EXPERIMENTAL:

Uranium oxides were converted to U_3O_8 by heating at 1023 K for 4 hours before use. Chlorination experiments were carried out at 973 K under an argon atmosphere, in which humidity and oxygen impurity were continuously kept less than 1 ppm. Chlorine gas was purged for half an hour after U_3O_8 addition to the chloride melts. The solution phase was separated from undissolving solid phase by using a glass filter which was attached at the end of the tube. Argon gas was purged to exchange chlorine gas dissolving in molten salt phase before the phase separation. Uranium concentration in molten salt phase was measured by hydrogen peroxide process. Molten salts used were LiCl, CsCl, RbCl, LiCl-KCl, LiCl-RbCl, NaCl-KCl, NaCl-RbCl, NaCl-KCl, and NaCl-CsCl eutectics.

RESULTS:

After 3.0 g U_3O_8 was putted into 3.1g LiCl-KCl eutectic melt at 973 K, chlorine gas was purged through the melts for over 1 hour at 20 ml/min.

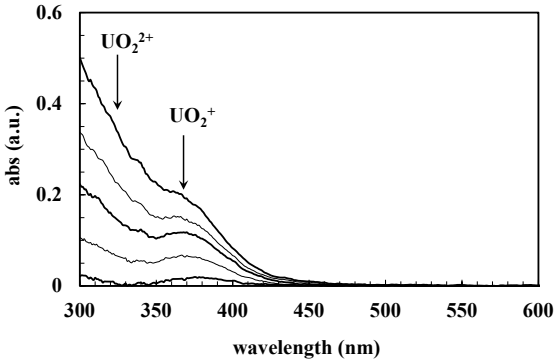

Fig. 1 . UV-Vis absorption spectra of uranium samples used in chlorination experimental (concentration depencence).

U_3O_8 was oxidized and dissolved into molten salt phase by chlorine gas as Eq. (1).

$$U_3O_8 + 3\,Cl_2 \rightarrow 3\,UO_2Cl_2 + O_2 \quad (1)$$

In order to analyse the valence of the uranium ions in the salts, UV-Vis absorption spectrum [1] was measured after the dilution of the salt by LiCl-KCl eutectic (Fig. 1). Absorption peak at 370 nm corresponding to UO_2^+ as well as the peak at < 330 nm corresponding to UO_2^{2+} were observed. The concentration of UO_2^+ formed was calculated to be < 5% of total uranium concentration. It is suggested that UO_2^{2+} was partially reduced by Ar gas due to the shift of the equilibrium potential in the melt as Eq. (2).

$$UO_2Cl_2 \rightarrow UO_2Cl + 1/2\,Cl_2 \quad (2)$$

Concentration of uranium ion in molten salt phase was measured by hydrogen peroxide method. The solubility of uranium in various molten salt was plotted as a function of melting point of the salts as shown in Fig. 2. The solubility of uranium in LiCl-KCl eutectic was 15.3 mol%, which was rather lower than that in NaCl-CsCl eutectic (37 mol%), RbCl melt (34 mol%). It was found that the solubility in CsCl was the highest in the molten salt tested. It is suggested that the solubility of uranium was not depended on the melting point of the molten salts but increased with increase of ionic diameter of alkali metal ion.

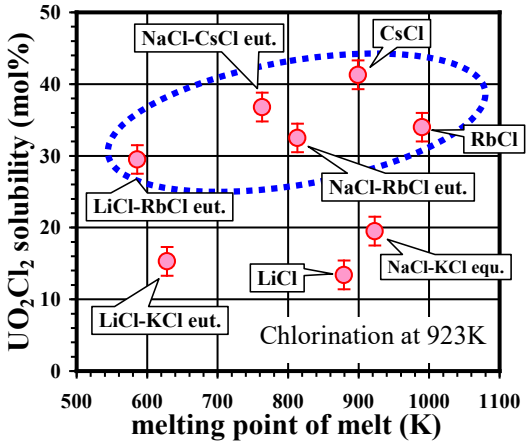

Fig. 2. Solubility of UO_2^{2+} depended on the melting point of the alkali chlorides.

REFERENCES

[1] Nagai, et al., J. Nucl. Sci. Techol. 41(2004) 690–695.

PR5-4 A Study on the Separation of Aluminum from Actinides in LiCl-KCl Eutectic Melt

Y. Sakamura, M. Iizuka, K. Uozumi, A. Uehara[1] and T. Fujii[1]

Central Research Institute of Electric Power Industry

[2]*Research Reactor Institute, Kyoto University*

INTRODUCTION: Electrorefining in molten LiCl-KCl eutectic-based salts is the key separation step in the pyrochemical treatment of spent nuclear fuels. It has been reported that the Al cathode is suitable for collecting actinides in the form of intermetallic compounds with a high separation factor against rare-earth fission products [1]. However, how to separate actinides from Al becomes problematic because U cannot be separated from Al by the anodic dissolution of U-Al alloy [2]. In this study, the behavior of Al^{3+} in LiCl-KCl eutectic melt was investigated to develop the separation technique of Al from Al-actinides intermetallic compounds.

EXPERIMENTS: LiCl-KCl eutectic melt was contained by a high-purity Al_2O_3 crucible in the temperature range 723-773 K, where a working electrode of W, Ta, Fe, Ni or Cu wire (1 mm diameter), a counter electrode of Al rod (3 mm diameter), a Ag/AgCl reference electrode and a type-K thermocouple were placed. The Ag/AgCl elec-trode consisted of a Ag wire immersed in a LiCl-KCl eutectic salt mixture with 1 wt% AgCl, which was con-tained in a closed-end Pyrex tube. The potential of the Ag/AgCl electrode was 2.410 V against a Li metal elec-trodeposited on a Ni wire. The concentration of Al^{3+} in the melt was changed by adding $KAlCl_4$ (APL Engi-neered Materials, 99.9% purity). The Al^{3+} concentration was determined by taking samples from the melt fol-lowed by ICP-AES analysis. All the measurements were conducted in a high-purity Ar atmosphere glove box (H_2O, O_2 < 1 ppm).

RESULTS: It is known that aluminum chloride has high vapor pressure. Figure 1 shows that the Al^{3+} concentration gradually decreased with time, which is probably due to the evaporation of $AlCl_3$ or Al_2Cl_6 from the melt. The evaporation rates of Al at 773 and 723 K were evaluated to be 5 x 10^{-5} and 1 x 10^{-5} g/cm^2/h, respectively when the Al^{3+} concentration was 0.15 mol%. Hence, Al^{3+} can be spontaneously removed from LiCl-KCl melts containing actinide chlorides. It is necessary to examine how long it takes to reduce the Al^{3+} concentration to a sufficiently low level.

Cyclic voltammograms (CVs) of various metal wire electrodes (W, Ta, Fe, Cu and Ni) were measured in LiCl-KCl eutectic melts with dissolved $KAlCl_4$ to investigate deposition behaviors of Al at the cathode. On the W electrode, as shown in Fig. 2, a cathodic current rises at about -1.0 V, which corresponds to the deposition of pure Al metal. The sharp anodic peak at -0.95 V is due to the dissolution of the deposited Al metal. The redox potential of Al/Al^{3+} on the W electrode is consistent with the CV of Al metal previously obtained in a LiCl-KCl-UCl_3 melt [2]. There is no other distinct peak, which indicates that W hardly forms alloys with Al under the condition of this measurement. The deposition behaviors of Al on Ta and Fe were similar to that of W.

The CV of Cu has a cathodic peak at -0.90 V and an anodic peak at -0.75 V, which correspond to the formation and decomposition of an Al-Cu alloy, respectively. The anodic peak at -0.65 V might be due to a different Al-Cu alloy with less Al activity. The anodic current rising at -0.40 V is due to the dissolution of Cu into the melt in the form of Cu^+ ion. It is suggested that Al can be separated from U by using a Cu electrode in LiCl-KCl melts containing Al^{3+} and U^{3+} because of the underpotential deposition of Al. The CV of Ni has an anodic peak at -0.45 V, which corresponds to the decomposition of an Al-Ni alloy. Since the cathodic current for the underpotential deposition of Al is small, the formation reaction of Al-Ni alloy might proceed slowly though the Al-Ni alloy is thermodynamically more stable than the Al-Cu alloy.

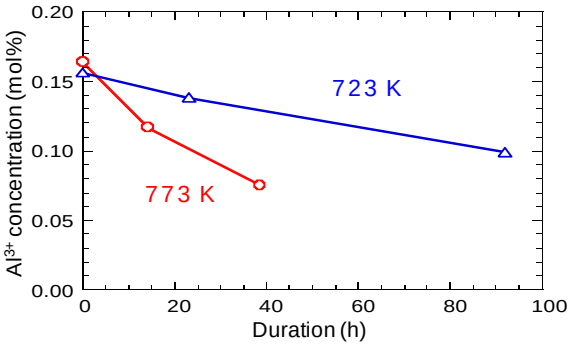

Fig. 1 Decrease in Al^{3+} concentration in melt with time.

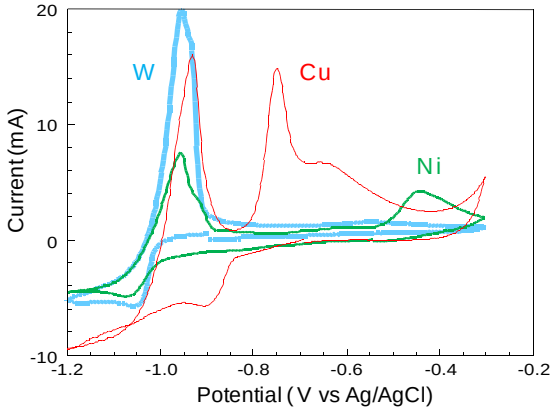

Fig. 2 CVs of W (ϕ1x5 mm), Ni (ϕ1x5 mm) and Cu (ϕ1x7 mm) electrodes in LiCl-KCl-$KAlCl_4$ (0.099 mol%-Al) with scan rate of 0.1 V/s at 724 K.

REFERENCES:

[1] P. Soucek *et al.*, *Proc. Int. Conf. Global 2009*, pp. 1156, Paris, France, Sept. 6-11, 2009.

[2] Y. Sakamura *et al.*, *KURRI Progress Report 2012*, pp. 100.

PR5-5 Electrochemical Behavior of Zirconium in Molten Alkali Chlorides

H. Matsuura, T. Emori, K. Nakamura, T. Uchiyama, T. Fujii[1] and A. Uehara[1]

Faculty of Engineering,Tokyo City University
[1]Research Reactor Institute, Kyoto University

INTRODUCTION: After the Fukushima Daiichi Nuclear Power Plant Accident, the reactor core has been experienced by high temperature from strong decay heat and leaded to fuel debris. The fuel debris may be expected to be the mixture of nuclear fuel, zircalloy theath, austenite stainless steel vessel, B_4C control blade and cement stuctural material. Especially, fuel material fisrt has contacted to zircalloy and resulted in uranium – zirocnium oxide solid solution (corium). For the completion of decomissioning process, these heavily fuel contaminated materials should be properly treated and stablized in some ways. One of ideal options is pyrometallurgical process, which has simplicity and compactness feature. Our proposed process consists to fluorination and molten salt electrolysis. In this process, uranium is expected to be selectively fluorinated, dissolved into molten salts and electro-reduced into metallic form. However, the behavior of zirconium in solid solution is unpredictable in each process, thus fluorination behavior of uranium - zircomium oxide has been firstly investigated [1]. Here, the electrochemical measurement of zircomium in molten LiCl-KCl has been carried out for the first step of the elucidation of electrochemical behavior containing zircomium.

EXPERIMENTAL: The molten salt was prepared by the mixing LiCl – KCl eutectic and $ZrCl_4$ powder (0.5w/o) (AAPL) in a quartz cell. Three electrodes were used for electrochemical measurement; working electrode: a tungsten wire in 1mmϕ, counter electrode: a pyrographite rod in 3mmϕ and reference electrode: a silver wire dipped to LiCl – KCl - AgCl molten salt in borosilicate glass. To avoid from the contamination of oxygen and moisture, all electrochemical measurements have been performed in an argon circulated glove box (Mbraun) and electroanalyser (Hokuto Denko). In this year, cyclic voltammetry has been carried out at 550 ^oC.

RESULTS and DISCUSSION: Figure 1 shows variated cyclic voltammograms depending on voltage sweep region. As shown in Fig. 1, large reduction current at -1.13 V *vs*. Ag^+/Ag is attributed to reduction to zirconium metal, which is relatively close to the decomposition of molten LiCl-KCl bath (it starts at ca. -1.25 V). This fact implies that zirconium would be difficult to selectively electoreduced in molten LiCl-KCl depending on the concentration of zircomium. Figure 2 shows sweep rate dependence of cyclic voltammograms. With increasing sweep rate, elecroreduction potential of zirconium is negatively shifted but electrooxidation potential of zirconium is almost independent to the sweep rate. This trend is typical semi-reversible reaction, which also implies difficulty of selective reduction of zircomium in LiCl-KCl.

In the next step, to be widen the reduction potential difference between zirconium and one of the elements of bath, two direction have been proposed, 1) to change the alternative molten chloride bath (NaCl-KCl and NaCl-2CsCl) or 2) to add small amount of fluoride in LiCl-KCl bath.

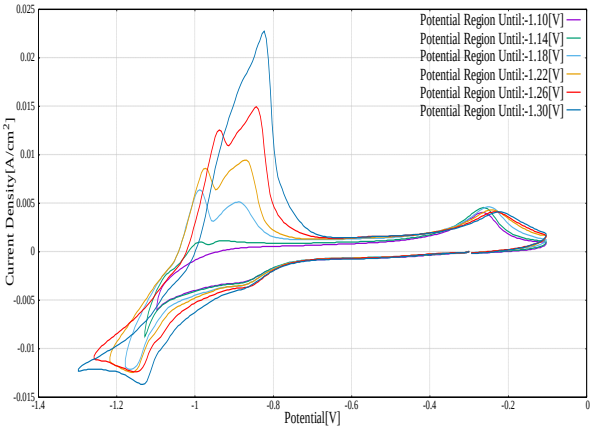

Fig. 1. Cyclic voltammograms of LiCl-KCl-ZrF_4(0.5w/o). Sweep rate: 100 mV/s

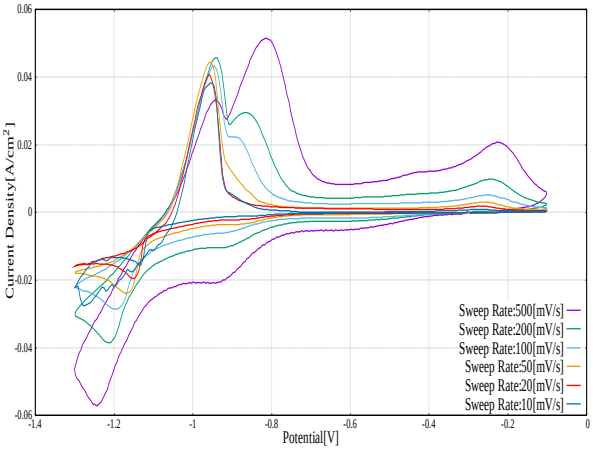

Fig. 2. Sweep rate dependence of cyclic voltammograms of LiCl-KCl-ZrF_4(0.5w/o).

This study is financially aided by the JSPS KAKENHI (15K0665).

REFERENCES:

[1] H. Matsuura *et al.*, NuMat2014, Clearwater beach, Florida, USA

PR5-6 Stability of Uranyl Ion in Aqueous Solutions of LiCl

N. Ohtori, N. Sato[1], Y. Ishii[1], A. Uehara[2], T. Fujii[2]

Department of Chemistry, Niigata University
[1]Graduate School of Science and Technology, Niigata University
[2]Research Reactor Institute, Kyoto University

INTRODUCTION: Recently, hydrate melts such as concentrated alkali halide aqueous solutions attract some attention as one of the novel candidates for solvents useful for reprocessing of spent nuclear fuels[1]. We performed molecular dynamics (MD) simulation of LiCl aqueous solutions containing uranyl ion and reported some results such as diffusion coefficients and average local structure around uranyl ion in the previous report[2]. Furthermore, we have analyzed coordination structure around uranyl ions in 14 M LiCl aqueous solution in more detail and compared the results with experimental results[3]. In this work, in order to discuss the stability of uranyl ion in hydrate melts, we have evaluated the Helmholtz free energy changes for the successive additional processes of chloride ion to uranyl ion in aqueous solutions of LiCl with various concentrations.

CALCULATION: MD calculation has been performed under *NVE* ensemble. The SPC/E model was used for water molecule. The other parameters were taken from the references cited in [3]. The water and uranyl molecules were constrained by SHAKE algorithm. The number of particles included in the simulation cell is shown in Table 1. Time step was 1.0 fs. The Helmholtz free energy changes have been evaluated by both free energy perturbation (FEP) method and thermodynamic integration (TI) method. The successive additional processes denoted by R1, R2, R3, and R4 are as follows:

$$UO_2^{2+} + Cl^- \rightarrow UO_2Cl^+ \quad \cdots \text{R1}$$
$$UO_2Cl^+ + Cl^- \rightarrow UO_2Cl_2 \quad \cdots \text{R2}$$
$$UO_2Cl_2 + Cl^- \rightarrow UO_2Cl_3^- \quad \cdots \text{R3}$$
$$UO_2Cl_3^- + Cl^- \rightarrow UO_2Cl_4^{2-} \quad \cdots \text{R4}$$

RESULTS: Figure 1 shows the free energy change as a function of distance between uranyl ion and chloride ion, which compares the results from both the results. First of all, we can see both the methods give the same results within the statistical errors. The minimum around 3-3.5Å means the most stable position within the first coordination shell. The maximum around 4-4.5Å means the energetic barrier caused by the first coordination shell. Figure 2 shows free energy changes for the successive additional processes from R1 to R4, which suggests that the most stable ionic species including uranyl ion is $UO_2Cl_4^{2-}$, regardless of the concentrations.

Table 1 Number of particles included the simulation cell for aqueous solutions of LiCl containing uranyl ion and the density of the simulated systems.

$[Cl^-]$ / mol dm^{-3}	d / kg cm^{-3}	Number of unit		
		H_2O	$UO_2^{2+}Cl^-_2$	Li^+ Cl^-
14	1.301	782	1	280
8	1.173	926	1	158
3	1.067	1044	1	58
0	1.001	1000	1	2

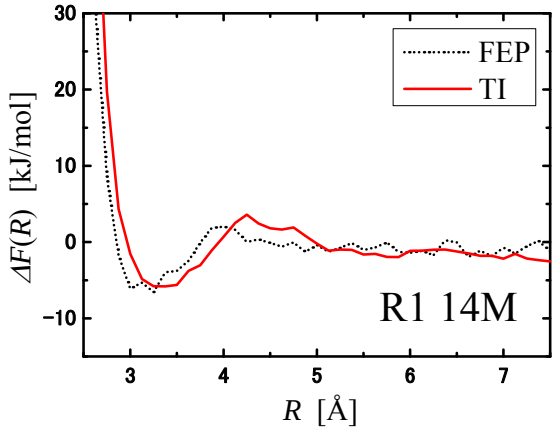

Fig.1 Free energy change for the additional process of Cl^- to UO_2^{2+} (R1) as a function of the coordination distance.

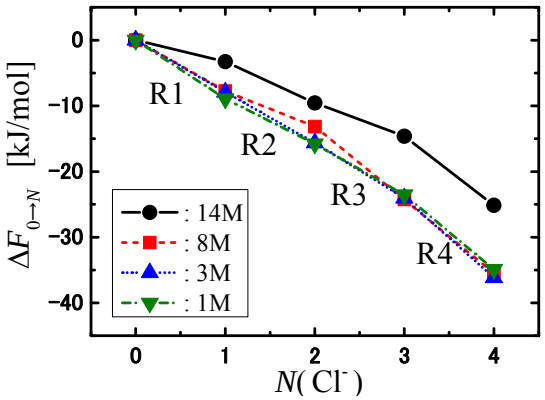

Fig.2 Free energy change for the successive additional processes of Cl^- to uranyl ion as a function of the coordination number of Cl^- by TI method.

REFERENCES:

[1] A. Uehara, O. Shirai, T. Fujii, T. Nagai and H. Yamana, *J. Appl. Electrochem.*, **42**, 455(2012).
[2] N. Ohtori, Y. Ishii, Y. Nagata, A. Uehara, T. Fujii, H. Yamana, K. Minato and Y. Okamoto, KURRI Progress Report 2012, PR2-1(2013).
[3] N. Ohtori, Y. Ishii, A. Uehara, T. Fujii, H. Yamana, and Y. Okamoto, KURRI Progress Report 2013, PR1-12(2014)

27P5-8

PR5-7 Study of Isotope Separation of Strontium and Calcium via Chemical Exchange Reaction

R. Hazama, Y. Sakuma[1], T. Yoshimoto, T. Fujii[2], S. Fukutani[2] and Y. Shibahara[2]

Graduate School of Human Environment, Osaka Sangyo University

[1]Research Laboratory for Nuclear Reactors, Tokyo Institute of Technology,

[2]Research Reactor Institute, Kyoto University

INTRODUCTION: Calcium is congener of strontium and easy to handle to check the isotope effects. By utilizing chemical separation method for calcium isotope effect in liquid-liquid extraction, we can evaluate the ratios between the field shift effect to the mass effect.

EXPERIMENTS: Isotopic enrichment occurs according to the following chemical exchange reaction:

$^{40}Ca^{2+}_{(aq)} + {}^{48}CaL^{2+}_{(org)} \rightarrow {}^{48}Ca^{2+}_{(aq)} + {}^{40}CaL^{2+}_{(org)}$ (1) where L represents macrocyclic polyether(18-crown-6).

ε /△M [×10^{-5}]	Method and system	Temp. (℃)	Ref.
51~17 (Sr)	Liquid-liquid extraction (LLE) with dicyclohexano-18-crown-6 (DC18C6). 2.3M-0.5M Sr in aqueous phase.	20±0.5	[1]
0.31 (Sr)	Cation-exchange chromatography with Sr lactate.	25±0.2	[2]
0.29 (Sr)	Cation-exchange chromatography with Sr acetate.	25±0.2	
0.10 (Sr)	Cation-exchange chromatography with Sr chloride.	25±0.2	
100 (Ca)	LLE with DC18C6. 0.07M $CHCl_3$	25	[3]
0.5~0.4 (Ca)	Solid-liquid chromatography(SLC)with ion exchange resin (Dowex50B)	—(Not specified)	[4]
3.7 (Ca)	SLC with ion exchange resin (Dowex1,50).	—	[5]
5.3 (Ca)	SLC with ion exchange resin (Dowex50W).	—	[6]
11 (Ca)	SLC with ion exchange resin (Dowex) with NH_4 α-hydroxyisobutyrate	—	[7]
51 (Ca)	SLC with ion exchange resin (ANKB-50) with iminodiacetate	—	[8]
13~87 (Ca)	SLC with ion exchange resin (PK-1) with counter-current	24-82	[9]
2~5.2 (Ca)	SLC with ion exchange resin (Asahi LS-6)	25	[10]
12 (Ca)	SLC with ion exchange resin (AG50WX4)	25	[11]
88 (Ca)	SLC with crown-ether resin (18C6, dimethylsulfoxide)	88	[12]
45 (Ca)	SLC with crown-ether resin (benzo-18C6). 9M HCl (0.8mmφ,1m)	35	[13]
38 (Ca)	SLC with crown-ether resin (benzo-18C6). 9M HCl (0.8mmφ,200m)	35	
75 (Ca)	SLC with crown-ether resin (benzo-18C6). Methanol	25	[14]
48 (Ca)	SLC with crown-ether resin (benzo-18C6). Ethanol/HCl mixed	40	[15]
13~24 (Ca)	Ion Exchange Electromigration	20,25, 40	[16]
150 * (Ca)	LLE with DC18C6 0.07M $CHCl_3$	20	This work
175 * (Ca)	LLE with DC18C6 0.07M $CHCl_3$	2	This work

Table 1. Unit mass enrichment factors of Sr and Ca isotope separation.*: Preliminary

RESULTS: Unit mass enrichment factors of Sr and Ca isotope separation are summarized in Table 1. In general, a crown ether gives a large separation factor with more than ten times, compared with an ion exchange method and has an applicable ability of separation in reality.

REFERENCES:

[1]K.Nishizawa *et al.*,J.Nucl.Sci.Technol., **32**(1995)1230.
[2] T. Oi *et al*., Sep. Sci. Technol., **27** (1992) 631.
[3]B.E. Jepson *et al*., J. Inorg. Nucl. Chem.**38**(1976)1175.
[4]G.D. Klinskii *et al*., Russ.J.Phys.Chem. **48**(1974) 659.
[5]D.A. Lee, J. Inorg. Nucl. Chem. **38**(1976) 161.
[6]W.A. Russell *et al*., Anal. Chem. **50**(1978)1151.
[7]J. Aaltonen, J. Suomen Kemi **B44**(1971)1.
[8]V.V.Gutsykov *et al*., Russ.J.Phys.Chem.**55**(1981)1667.
[9]N. Kobayashi, J. Chromatogr. **252**(1982)121.
[10] T. Oi *et al*., Sep. Sci. Technol., **28** (1993) 1971.
[11]B.E.Jepson *et al*., Sep. Sci. Technol., **22** (1984) 1029.
[12]B.E.Jepson *et al*., Sep. Sci. Technol., **28**(1993) 507.
[13]S.Umehara *et al*.,Prog.Theor.Exp.Phys.**2015**,053C03.
[14]S.Nemoto *et al*.,Isotopes Envir.Heal.Stu.**49**(2013)257
[15]S. Okumura *et al*., J. Chromatogr. **A1415**(2015)67.
[16]Y. Fujii *et al*.,Z. Natureforsch, **40a** (1985) 843.

PR5-8

Disproportionation Reaction of RE(II) (RE = Nd, Dy, Pr) in $CaCl_2$-LiCl Eutectic Molten Salt

H. Sekimoto, A. Uehara[1] and T. Fujii[1]

Faculty of Engineering, Iwate University
[1]Research Reactor Institute, Kyoto University

INTRODUCTION: Mutual separation of Nd, Dy and Pr is essentially important for the recycling of the neodymium magnet. Uehara et al. reported on the mutual separation of La and Nd utilizing the disproportionation reaction of Nd(II) to metallic Nd and Nd(III) in LiCl-KCl molten salt [1]. This technique seems quite attractive comparing with the conventional processes such as the ion exchange process and the solvent extraction process in terms of the environmental load. In this study, the formation of Nd(II), Dy(II) and Pr(II) in $CaCl_2$-LiCl eutectic molten salt was investigated with the combination of the absorption spectroscopy and the galvanostatic electrolysis method.

EXPERIMENTS: Regents of $CaCl_2$, LiCl, $NdCl_3$, $DyCl_3$, and $PrCl_3$ was weighed and inserted into a optical cell attached with a cylindrical quartz tube and melted at 700 °C to form $RECl_3$(RE = Nd, Dy, Pr)-$CaCl_2$-LiCl molten salt. The galvanostatic electrolysis at -10 mA was conducted with 3 electrodes; the working electrode was a tungsten wire of 1 mm diameter, the counter electrode and the reference electrode was a silver wire of 0.5 mm diameter which was immersed in 1 mol%AgCl-$CaCl_2$-LiCl molten salt held in a cylindrical pyrex glass tube. The counter electrode and the reference electrode was electrically contacted with the $RECl_3$-$CaCl_2$-LiCl molten salt through the thin pyrex glass film. All potentials in this paper were measured against the Ag/AgCl(1 mol%) electrode. The absorption spectra of the $RECl_3$-$CaCl_2$-LiCl molten salt was measured by UV-Vis absorption spectrometer with the reported procedure [2].

RESULTS: The cathodic potential during the galvanostatic electrolysis was as follows; -1.67 V for the $NdCl_3$-$CaCl_2$-LiCl molten salt, -1.50 V for the $DyCl_3$-$CaCl_2$-LiCl molten salt and -1.80 V for the $PrCl_3$-$CaCl_2$-LiCl system. The absorption spectra shown in Fig. 1 (a) and (b) indicates that Nd(II) and Dy(II) formed during the galvanostatic electrolysis in the $NdCl_3$-$CaCl_2$-LiCl molten salt and $DyCl_3$-$CaCl_2$-LiCl molten salt, respectively. On the other hand, the existence of Pr(II) was not confirmed in the absorption spectra shown in Fig.1 (c). Consequently, the following reactions proceeded during the galvanostatic electrolysis.

$$Nd(III) + e \rightarrow Nd(II) \quad (1)$$
$$Dy(III) + e \rightarrow Dy(II) \quad (2)$$
$$Pr(III) + 3e \rightarrow Pr \quad (3)$$

As shown in Fig. 1 (a), the absorption peak attributing Nd(II) diminished in 10 min. after the electrolysis, which indicates that Nd(II) decomposed through the disproportionation reaction.

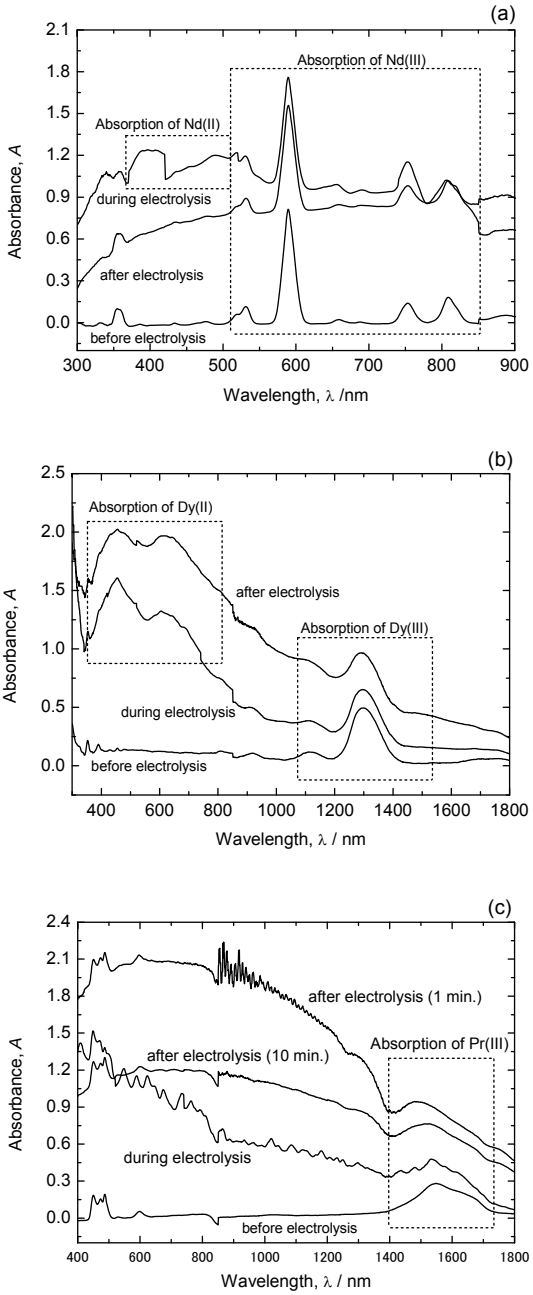

Fig. 1. Absorption spectra before, during and after the galvanostatic electrolysis at -10 mA for (a) $NdCl_3$-$CaCl_2$-LiCl molten salt, (b) $DyCl_3$-$CaCl_2$-LiCl molten salt and (c) $PrCl_3$-$CaCl_2$-LiCl molten salt.

REFERENCES:

[1] A. Uehara, K. Fukasawa, T. Nagai, T. Fujii, and H. Yamana, *J. Nuclear Mater.*, **414**, 336 (2011).

[2] H. Sekimoto, A. Uehara, T. Fujii, H. Yamana, KURRI Progress report, (2014).